Brain Stimulation 15 (2022) 458–471

Contents lists available at ScienceDirect

Brain Stimulation

journal homepage: http://www.journals.elsevier.com/brain-stimulation

Daily prefrontal closed-loop repetitive transcranial magnetic stimulation (rTMS) produces progressive EEG quasi-alpha phase entrainment in depressed adults

Josef Faller [a, 1], Jayce Doose [b, 1], Xiaoxiao Sun [a, c, 1], James R. Mclntosh [a, d], Golbarg T. Saber [e, f], Yida Lin [g], Joshua B. Teves [e], Aidan Blankenship [e], Sarah Huffman [h], Robin I. Goldman [i], Mark S. George [h, j], Truman R. Brown [b, e], Paul Sajda [a, k, l, m, *]

[a] Department of Biomedical Engineering, Columbia University, New York, NY, 10027, USA
[b] Center for Biomedical Imaging, Medical University of South Carolina, Charleston, SC, 29425, USA
[c] US DEVCOM Army Research Laboratory, Aberdeen Proving Ground, MD, 20115, USA
[d] Department of Orthopaedic Surgery, Columbia University Irving Medical Center, New York, NY, 10032, USA
[e] Department of Radiology and Radiological Science, Medical University of South Carolina, Charleston, SC, 29425, USA
[f] Department of Neurology, University of Chicago, Chicago, IL, 60637, USA
[g] Department of Computer Science, Columbia University, New York, NY, 10027, USA
[h] Department of Psychiatry and Behavioral Sciences, Medical University of South Carolina, Charleston, SC, 29425, USA
[i] Center for Healthy Minds, University of Wisconsin-Madison, Madison, WI, 53705, USA
[j] Ralph H. Johnson VA Medical Center, Charleston, SC, 29401, USA
[k] Department of Radiology, Columbia University Irving Medical Center, New York, NY, 10032, USA
[l] Department of Electrical Engineering, Columbia University, New York, NY, 10027, USA
[m] Data Science Institute, Columbia University, New York, NY, 10027, USA

ARTICLE INFO

Article history:
Received 3 August 2021
Received in revised form
31 January 2022
Accepted 17 February 2022
Available online 26 February 2022

Keywords:
Closed-loop neurostimulation
Electroencephalography (EEG)
Repetitive transcranial magnetic stimulation (rTMS)
Inter-trial phase coherence (ITPC)
Major depressive disorder (MDD)

ABSTRACT

Background: Transcranial magnetic stimulation (TMS) is a non-invasive neuromodulation modality that can treat depression, obsessive-compulsive disorder, or help smoking cessation. Research suggests that timing the delivery of TMS relative to an endogenous brain state may affect efficacy and short-term brain dynamics.

Objective: To investigate whether, for a multi-week daily treatment of repetitive TMS (rTMS), there is an effect on brain dynamics that depends on the timing of the TMS relative to individuals' prefrontal EEG quasi-alpha rhythm (between 6 and 13 Hz).

Method: We developed a novel closed-loop system that delivers personalized EEG-triggered rTMS to patients undergoing treatment for major depressive disorder. In a double blind study, patients received daily treatments of rTMS over a period of six weeks and were randomly assigned to either a synchronized or unsynchronized treatment group, where synchronization of rTMS was to their prefrontal EEG quasi-alpha rhythm.

Results: When rTMS is applied over the dorsal lateral prefrontal cortex (DLPFC) and synchronized to the patient's prefrontal quasi-alpha rhythm, patients develop strong phase entrainment over a period of weeks, both over the stimulation site as well as in a subset of areas distal to the stimulation site. In addition, at the end of the course of treatment, this group's entrainment phase shifts to be closer to the phase that optimally engages the distal target, namely the anterior cingulate cortex (ACC). These entrainment effects are not observed in the group that is given rTMS without initial EEG synchronization of each TMS train.

* Corresponding author. Department of Biomedical Engineering; Department of Radiology; Department of Electrical Engineering; Data Science Institute, Columbia University, United States.
E-mail address: psajda@columbia.edu (P. Sajda).
[1] contributed equally.

https://doi.org/10.1016/j.brs.2022.02.008

Conclusions: The entrainment effects build over the course of days/weeks, suggesting that these effects engage neuroplastic changes which may have clinical consequences in depression or other diseases.

1. Introduction

Several forms of targeted neurostimulation can treat multiple diseases and psychiatric conditions [1–5]. An important issue for these approaches is how to focus the stimulation in both space (location) and time (relative to other brain events) [6–8]. This is particularly true in non-invasive neurostimulation such as TMS, where the ultimate therapeutic target site might be deep in the brain while the initial stimulation site is often located superficially. In the case of pharmacologically resistant major depressive disorder (MDD), the Food and Drug Administration (FDA) approved repetitive transcranial magnetic stimulation (rTMS) at 10 Hz over the left dorsolateral prefrontal cortex (DLPFC) as a treatment [5,9–11]. One of the earliest hypotheses held that rTMS might be an effective antidepressant because the proximal stimulation over DLPFC could cause changes in a circuit involving distal brain regions including the anterior cingulate cortex (ACC) and the subgenual ACC (sgACC), where these distal regions are believed to be linked to the disease state [12–14]. Evidence in support of this theory was reported by George and others [5,15].

The therapeutic mechanisms of TMS are thought to be mediated by connectivity between the stimulation site and deeper brain structures [16]. Functional imaging studies have observed significant functional connectivity between the ACC and DLPFC [17–20]. However, it is also well-known that functional connectivity can be dynamic, and thus the ability to affect distal regions via stimulation is likely impacted by these dynamics, i.e., the dose of the neurostimulation to the target area may depend on the timing of the rTMS to the stimulation site relative to the dynamics of the functional connectivity between the two sites.

A candidate for tracking the dynamics of the functional connectivity between the DLPFC and ACC is prefrontal alpha oscillation. Alpha oscillations have been implicated in network connectivity, with the phase of alpha linked to activation and release of inhibition across and within networks [19,21–24]. Alpha phase could therefore act as a gating mechanism where different phases in the cycle are associated with states of low and high excitability within the network. Hypothetically, there may be certain, potentially even subject-specific, phases in the alpha cycle where stimulation over DLPFC causes a greater effect at distal brain regions. This idea is consistent with research showing that the timing of stimulus onset relative to the phase of the alpha cycle influences perception [25–27].

An important and relatively under-explored question is whether it matters what phase the brain is in when a TMS pulse is delivered. Several groups have investigated synchronized TMS delivery to the alpha phase (or the mu/beta rhythm in the motor system) and have shown acute/transient effects suggesting that excitability is indexed by phase [28–30]. There are, however, ongoing debates, including over the size and anatomical location of effects [31–33]. All these studies assessed phase effects at relatively short time scales and have not examined effects of phase-synchronized rTMS applied over multiple weeks as part of a clinical intervention. Most have also studied the motor system and have used motor evoked potentials as their output marker. Notably, we have found in previous work that TMS-evoked BOLD response, particularly in the dorsal ACC, depends on the frontal alpha phase prior to TMS delivery [24,34]. The data we report here is part of a randomized, active-comparator controlled clinical trial in depression we are currently completing comparing phase dependent prefrontal TMS to the standard approach that does not take phase-dependence into account. The results from this clinical trial will show whether state-dependent, phase-locked stimulation may be more effective than conventional rTMS treatments.

In this paper, we consider whether phase dependent effects – entrainment – might persist across weeks when rTMS is synchronized to ongoing quasi-alpha (6–13 Hz) activity in the prefrontal cortex. Note that we have defined quasi-alpha as a slightly expanded bandwidth version of the traditional definition of alpha (8–12 Hz) due to early system tests trying to maximize prefrontal signal and be inclusive of more subjects (see Discussion section). We developed a novel closed-loop neurostimulation system (see Fig. 1) and used it to test the hypothesis that synchronized application across weeks of rTMS treatment might yield increased entrainment, as observed by the EEG dynamics after stimulation. We assessed entrainment using the inter-trial phase coherence (ITPC) measure, which is a metric to capture how consistent oscillatory phase is across an ensemble of event-locked trials [35,36], and examined how this measure changes over a period of weeks as rTMS is periodically applied either synchronized or unsynchronized to the preferred prefrontal quasi-alpha phase of an individual.

We investigated this hypothesis in a group of MDD patients as part of an ongoing double-blind clinical study, where one group receives rTMS synchronized to their quasi-alpha activity (SYNC), while another group receives the same stimulation, but the initial pulse in each train is not synchronized (UNSYNC). The phase at which we synchronized the first pulse in each TMS pulse train is based on a unique targeting approach using an integrated fMRI-EEG-TMS (fET) system (see Refs. [24,34,37] and supplemental material; another separate manuscript about the fET system is also in preparation [38]), where the preferred prefrontal alpha phase φ_{pre} is the phase which yielded the strongest BOLD fMRI activation in the ACC. The method used to estimate φ_{pre} is described in the Materials and Methods section and the supplementary material (see S.1 in supplementary material for details). In this report, we focus on whether rTMS applied synchronized or unsynchronized to this preferred phase over 30 sessions of treatment impacts entrainment over time.

2. Materials and methods

2.1. Subjects

This is an interim blinded analysis of an ongoing clinical trial. All EEG data for this randomized, double-blind, active comparator-controlled clinical trial (ClinicalTrials.gov ID: NCT03421808) was collected at the Medical University of South Carolina, SC, USA. 23 patients were consented and enrolled in the study, and 15 (see Table 1) were able to complete the rTMS treatment. 8 subjects dropped out for reasons including claustrophobia (N = 2, i.e., could not complete MRI), hospital admission due to severe depressive episodes (N = 1), and some participants could no longer make the time commitment for the study (N = 5). During enrollment, all

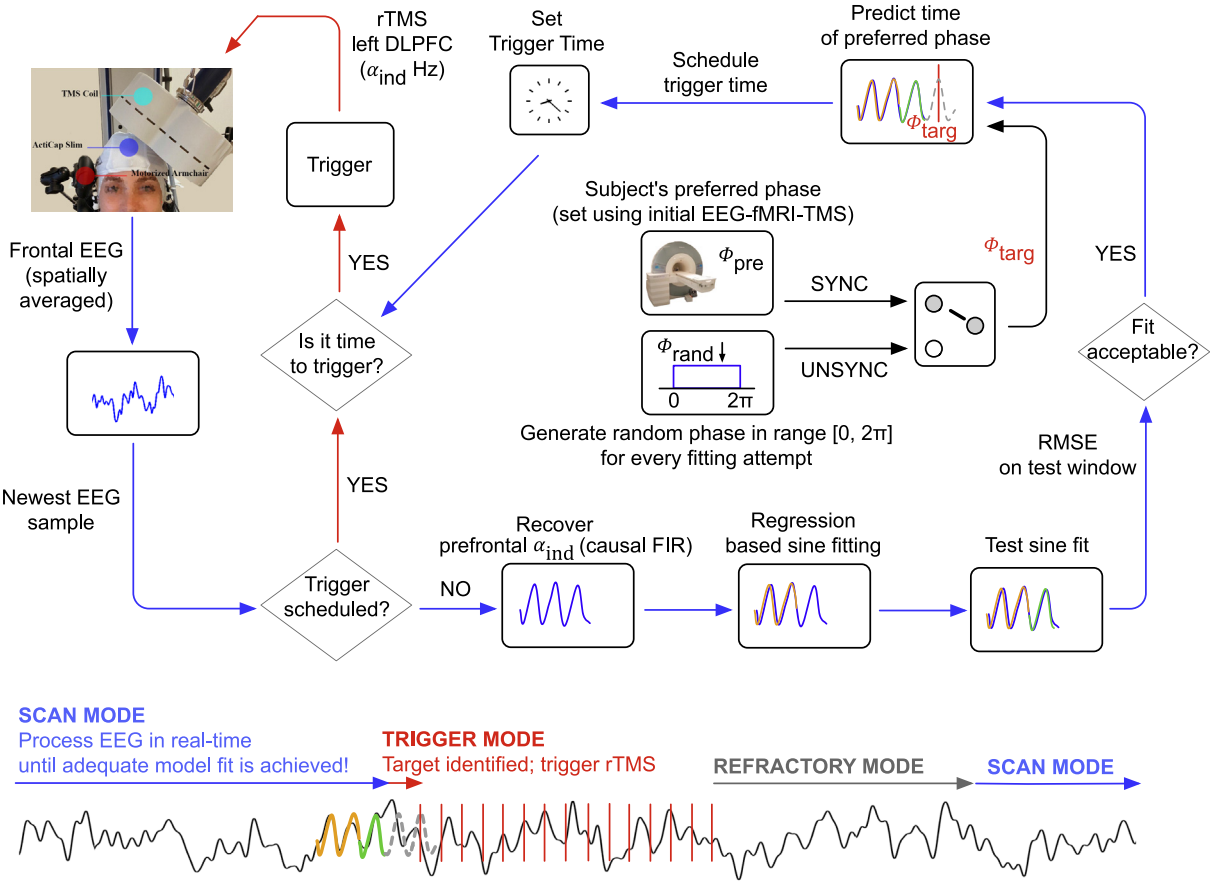

Fig. 1. Logic of the closed-loop stimulation system that synchronizes the onset of rTMS to EEG alpha phase. The system continuously processes EEG in real-time, where the EEG is sampled at 10 kHz. To optimize throughput, data is read from the amplifier in chunks of 20 data points (i.e., samples). Subsequently, a low-pass antialiasing filter is applied with a cut-off at 50 Hz and the signal is downsampled to 500 Hz. For EEG processing, the logic switches between three operation modes, SCAN MODE (blue arrows), TRIGGER MODE (red arrows) and REFRACTORY MODE (grey arrow). Model fitting in SCAN MODE is performed in parallel to reading new data (multi-threading) and every new fitting attempt is always performed on the newest available data. Starting in SCAN MODE, the system fits multiple single-sine function models on to the individual's prefrontal quasi-alpha signal (α_{ind}, 6–13 Hz; spatial average of FP1, F7 and F3) in a time window [-300, ~-100] ms relative to the newest EEG sample (see S.2 in supplementary material). The resulting model that achieves the lowest root mean square error (RMSE) on that training signal is used for prediction on a more recent test signal in the time window [-100, 0] ms, again relative to the newest EEG sample. If the RMSE on that test signal does not reach below a pre-determined, subject-specific threshold (see S.4 in supplementary material), the logic continues with a new fitting attempt, but now again using data relative to the newest EEG data that arrived in real-time. Otherwise, if and only if the RMSE on that test signal is below this threshold, the single-sine model is used to predict the prefrontal quasi-alpha wave up to 123 ms into the future. The targeted phase, φ_{targ}, then depends on the randomized treatment arm for that patient. For SYNC, φ_{targ} is the subject specific preferred phase φ_{pre} that was determined in an initial combined fMRI-EEG-TMS experiment (see S.1 in supplementary material). For UNSYNC, φ_{targ} is drawn from a uniform random distribution over the range $[0, 2\pi]$ at every prediction ($\varphi_{targ} \sim U(0, 2\pi)$). Taking into account the group delay of causal filtering and processing time, the logic then schedules the rTMS trigger onset at the predicted future time of φ_{targ} and switches into TRIGGER MODE. In TRIGGER MODE, no model fitting is attempted. Instead the logic keeps reading new data samples. Whenever the scheduled trigger time has arrived, a train of 40 TMS pulses is triggered where the inter-pulse-interval is the reciprocal of the subject's individual alpha frequency (IAF, $\Delta t_{ipi} = 1/IAF$). Directly after the 40^{th} pulse has been triggered, the logic switches into REFRACTORY MODE, where the system does nothing other than reading in new EEG samples for $2 \times 40 \times \frac{1}{IAF}$ or twice the amount of time it took to deliver 40 TMS pulses, after which the logic again switches into SCAN MODE. (For interpretation of the references to colour in this figure legend, the reader is referred to the Web version of this article.)

patients were randomly assigned to the SYNC or UNSYNC group before treatment. The inclusion criteria included diagnosis of unipolar MDD in a current major depressive episode, Hamilton Rating Scale for Depression (HRSD) score ≥ 20, age between 21 and 70, and fixed and stable antidepressant medications for 3 weeks prior to and during the trial. Patients also needed to show a moderate level of resistance to antidepressant treatment, defined as failure of one to four adequate medication trials, or intolerance to at least three trials. Primary exclusion criteria were that patients had to be able to undergo a 3T MRI scan as well as TMS treatment safely. To ensure that baseline level of depression severity was stable at the time of study enrollment, patients were dropped from the study if

Table 1
Number of patients in every group, average age, gender, and average (± standard deviation) duration of the current depressive episode in weeks are shown. The duration of the current depressive episode is used to describe how long an individual patient has been depressed during the present depressive episode. There is no significant difference between the SYNC and UNSYNC groups in age ($p = 0.480\ 3$) or duration of current depressive episode ($p = 0.703\ 4$).

	# of Patients	Age (y)	Sex	Duration of Current Depressive Episode
SYNC	7	50.1 ± 10.5	6 F, 1 M	50.1 ± 39.9 weeks
UNSYNC	8	45.0 ± 15.9	6 F, 2 M	60.6 ± 60.5 weeks
Total	15	47.4 ± 13.4	12 F, 3 M	55.7 ± 50.4 weeks

they showed more than 30% improvement in the HRSD score from the time of their initial screening to the baseline assessment. A full list of inclusion and exclusion criteria can be found on ClinicalTrials.gov. (https://clinicaltrials.gov/ct2/show/NCT03421808). This study was reviewed and approved by the Institutional Review Board of Medical University South Carolina and written informed consent was obtained from all study participants prior to enrollment.

2.2. EEG setup for closed-loop EEG-rTMS

Head circumference was used to select an appropriately sized cap with 32 active EEG sensors (ActiCap Slim, Brain Products GmbH, Munich, Germany; [39]), which was placed on the patient's head. Cap placement was verified by making sure the EEG sensor for channel Cz was located midway between nasion and inion as well as between the left and right preauricular points. Impedance was reduced to less than 10 $k\Omega$ for each electrode. EEG was sampled at 10 kHz using a biosignal amplifier (ActiChamp, Brain Products GmbH, Munich, Germany). This amplifier is designed to recover from electromagnetic artifacts related to a TMS pulse in less than 1 ms (see also [40]. No additional high-pass filters were applied before recording the data. Synchronized acquisition of all signals and experimental events was accomplished through the software framework Labstreaming Layer (LSL; see [41]) and all data was stored in extensible data format (XDF; [42]) files. Additional detailed information about the equipment setup and conduct with closed-loop EEG-rTMS system are available in S.1 to S.5 of the supplementary materials.

2.3. EEG preprocessing for post-hoc analysis

Prior to EEG analysis, a double exponential model was fit to the average post-pulse response from t = 17.5 ms to t = Δt_{ipi}, which is the interval between pulses in a train, i.e., 1/*IAF*. This fit was then subtracted from the post-pulse response for all pulses in a session in order to suppress a slow instantaneous TMS artifact present in the EEG. This instantaneous TMS artifact was interpolated from −1 ms to 17.5 ms. The entire EEG session was then low-pass filtered with a cut-off at 50 Hz and down-sampled to 250 Hz. Infomax-based Independent Component Analysis (ICA; see Ref. [43] was then performed on each session for each subject independently. The CORRMAP [44] plugin for the EEGLAB MATLAB toolbox [45] was used to identify ocular artifacts across sessions and those components were subsequently removed from the EEG data. For consistency with other studies in this project, data was then re-referenced to electrode location TP10 (close to the right mastoid). The arithmetic mean was computed separately for every EEG channel and subtracted from every point in the time series for that channel.

Next, EEG data was segmented into two separate datasets (**Pre** and **Post**) for two separate calculations (see Fig. 2 and Fig. 3). For dataset **Pre**, epochs were extracted from the intervals between two rTMS pulse trains. Only epochs of 2.5 s or longer were considered, and the longest epoch was 186.0 s long. The mean epoch length (interval between two rTMS pulse trains) was 15.6 s at a standard deviation of 75.3 s. For dataset **Post**, epochs were extracted from a time window $[0, 2.5]$ s relative to the last (i.e., 40^{th}) pulse of each pulse train. A band-pass filter (FIR, 6–13 Hz, order 63) was applied bi-directionally to attenuate oscillatory signal components at frequencies outside the alpha band [46].

2.4. Trial weighted inter-trial phase coherence

Inter-trial phase coherence (ITPC) is commonly used for quantifying event-related phase modulation [47]. ITPC is a scalar value that ranges from [0, 1] and is derived from an ensemble of phase values at a particular time point in trials. A value closer to 0 indicates low phase alignment among the trials at that particular time point, while an ITPC value closer to 1 indicates high alignment of phase angles across trials [45] at that point. As a simple example, if there is a systematic effect across *N* trials where at time point $t_{example}$ oscillatory activity shows similar phase (e.g., close to "peak" of a sine wave), we would expect for the single ITPC value we derive at time point $t_{example}$ for these *N* trials to be closer to 1 rather than 0. In order to identify effects most relevant to the rTMS treatment, we focused our analysis on electrodes at (F3) and adjacent to (FP1, F7) the stimulation site over DLPFC (the same channels were previously used to determine IAF).

The accuracy of the phase estimation of the Hilbert transform for each pulse train from each session is dependent on the signal to noise ratio (SNR) of each pulse train (the ratio of the quasi-alpha (6–13 Hz) wave to other EEG components (1–30 Hz)). This approximation based on fast Fourier transform (FFT) has errors in the energy sense due to the fact that Hilbert transformation is a unitary operator in the L^2 space [48,49], so instead of averaging across trials for the phase coherence calculation, each trial was first weighted by its power in the inter pulse train period (epoched dataset **Pre**; see Fig. 2). Relative power was used to calculate the trial weight of phase for each pulse interval with the consideration of consistency and comparability within one session. Relative power was defined as the ratio of absolute quasi-alpha power to the total power calculated from 1 to 30 Hz (spanning delta, theta, alpha and beta bands, see eq (2)). Quasi-alpha power was calculated as the integrated power between 6 and 13 Hz which is the range used to identify the IAF for each subject during the rTMS triggering. The power of the entire spectrum (1–30 Hz) was calculated by Welch's power spectral density (PSD) estimation method, for which the complete epoch was segmented into eight windows that overlapped 50%. The approximate integrals of absolute quasi-alpha power (6–13 Hz) and total frequency band (1–30 Hz) were calculated with the trapezoidal method of non-unit but uniform spacing which is determined by the frequency resolution (frequency resolution was 0.2441 Hz). More formally, trial weight was calculated as follows:

$$\alpha_{n,S} = \int_{6}^{13} P_{n,S,f}^{targeted} df = \int_{6}^{13} \frac{1}{3}\left(P_{n,S,f}^{FP1} + P_{n,S,f}^{F3} + P_{n,S,f}^{F7}\right) df \tag{1}$$

$$\bar{\alpha}_{n,S} = \frac{\alpha_{n,S}}{\int_{1}^{30} P_{n,S,f}^{targeted} df} \tag{2}$$

$$\omega_{n,S} = \frac{\bar{\alpha}_{n,S}}{\sum_{n=1}^{n=75} \bar{\alpha}_{n,S}} \tag{3}$$

where $\alpha_{n,S}$ is the absolute quasi-alpha power for trial n from session S; $\int_{f1}^{f2} P_{n,S,f}^{j} df$ is the integral of power between frequency $f1$ and $f2$ of channel j for trial n from session S, $j = \{FP1, F3, F7\}$; *targeted* refers to the near targeted area which includes FP1, F3, and F7; $\bar{\alpha}_{n,S}$ is the relative power for trial n from session S; $\omega_{n,S}$ is the trial weight for trial n from session S.

After the trial weight calculation, the Hilbert Transform($H\{\cdot\}$) was applied to the dataset **Post** (see Fig. 2) to estimate the instantaneous phase $\varphi_{n,j}(t)$ of signal $x_{n,j}(t)$ locked to the last TMS pulse for trial n and channel j, where $t \in [0, 2.5]$(s), $\varphi(t) \in [-\pi, \pi]$.

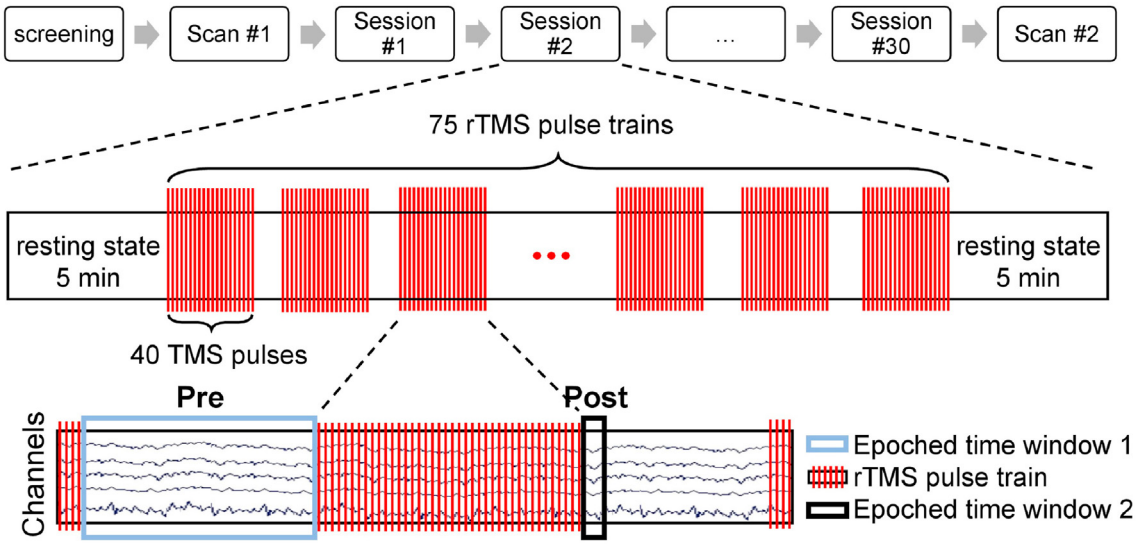

Fig. 2. Longitudinal treatment design. Before the pre-treatment scan (scan #1), all subjects were screened to meet all inclusion and exclusion criteria described in Materials and Methods section (see **Subjects** section for details). Then the first scan was done with the fET system to determine the pre-treatment preferred phase φ_{pre}, which was then used as the individual target phase φ_{targ} for subjects in SYNC group during the entire EEG-rTMS treatment. During the six to seven week treatment period, each subject received a total of 30 rTMS treatment sessions (one treatment each weekday). In each session, there were two 5-min rest periods (before the first and after the last pulse train). Each treatment consisted of 75 rTMS pulse trains/session (3000 pulses/session). In each rTMS pulse train, 40 TMS pulses were delivered at the IAF for each subject. Two datasets were split off from the EEG recordings during the treatment session: **Pre** was used for estimating the trial weight of each pulse train, **Post** was used for computing the post-stimulation trial weighted inter-trial phase coherence. After all treatment sessions, another scan (scan #2) was done with the fET system to obtain the post-treatment preferred phase φ_{post}.

$$\varphi(t) = arctan\left(\frac{H\{x(t)\}}{x(t)}\right), \quad \varphi(t) \in [-\pi, \pi] \tag{4}$$

We then transformed the phase angle back to the analytic signal $Z_{n,j}(t)$ in the real and complex domain using Euler's formula.

$$Z_{n,j}(t) = re^{i\varphi_{n,j}(t)} = rcos(\varphi_{n,j}(t)) + i \times rsin(\varphi_{n,j}(t)), \quad r = 1 \tag{5}$$

Our approach of calculating ITPC was slightly modified from the standard approach introduced by Ref. [36]. Instead of simply averaging $Z_{n,j}(t)$ across the trials (i.e., subscript n), we calculated a weighted average, where the analytic signal for each trial was weighted by coefficients $\omega_{n,S}$ that were derived based on relative quasi-alpha power for that trial, as described earlier (see Equation (3)). That way the absolute part of the intermediate result, $\bar{Z}_{j,S}(t)$, represented trial weighted ITPC for channel (electrode) j, which resulted in a 3 × 625 matrix of ITPC values for each session. Each row represents one channel (FP1, F3, and F7) and columns represent the samples in a trial (width of epoch of dataset **Post**, 2.5 s × 250 Hz sampling rate). Finally, for the spatial average, we calculate the circular mean across these three EEG channels and obtain the absolute value, which is the post-stimulation $ITPC_S(t)$ of the near target region. Based on these resulting time series, we determined the ITPC for the time range [0, 2.5]s post rTMS pulse train (see Fig. 3).

$$\bar{Z}_{j,S}(t) = \sum_{n=1}^{n=75} e^{i\times\varphi_{n,S,j}(t)} \times \omega_{n,S} \tag{6}$$

$$ITPC_S(t) = |\frac{1}{3}\sum_{j=1}^{j=3}\bar{Z}_{j,S}(t)| = |\frac{1}{3}\sum_{j=1}^{j=3}\sum_{n=1}^{n=75} e^{i\times\varphi_{n,S,j}(t)} \times \omega_{n,S}| \tag{7}$$

where $ITPC_S(t)$ refers to the average ITPC value for session S at time t post rTMS; $|\bar{Z}_{j,S}|$ refers to the ITPC value of channel j from session S; $\varphi_{n,S,j}(t)$ is the instantaneous phase of channel j from trial n of session S; $\omega_{n,S}$ is the trial weight for trial n of session S.

2.5. Correlation between first post-stimulation ITPC peak and treatment session

At the subject level, in order to see how this brain synchronization after an rTMS pulse train changes across sessions, Spearman correlation (Spearman's ρ) was used to capture the relationship between the first post-stimulation ITPC peak (referred to as $ITPC^{max}_{[1]}$, which is defined as the first local maximum of the ITPC following the last TMS pulse in a train, see Fig. 3 and the details of first peak detection are available in S.6 of the supplementary materials) and the treatment session number [50]. The range of Spearman's ρ is $[-1, 1]$, with 1 indicating perfect correlation, −1 perfect anticorrelation and 0 that there is no monotonic association between two variables [51].

2.6. Generalized linear mixed-effects model

We used a generalized linear mixed-effects model (GLMM) to analyze changes in $ITPC^{max[1]}$ across sessions as a function of treatment arm (SYNC vs UNSYNC). A GLMM is an extension to the generalized linear model (GLM) in which the linear predictor contains random effects in addition to the usual fixed effects [52]. The general form of a GLMM as per [53] is as follows:

$$y = X\beta + Z\mu + \epsilon \tag{8}$$

Where y is the outcome variable; X represents the predictor variables; β is a column vector of the fixed-effects regression coefficients; Z is the design matrix for the random effects (the random complement to the fixed X); μ is a vector of the random effects (the random complement to the fixed β); and ϵ is a column vector of the residuals.

We used the GLMM in Matlab (Statistics and Machine Learning Toolbox, Matlab 2018b, Mathworks, USA) to investigate the

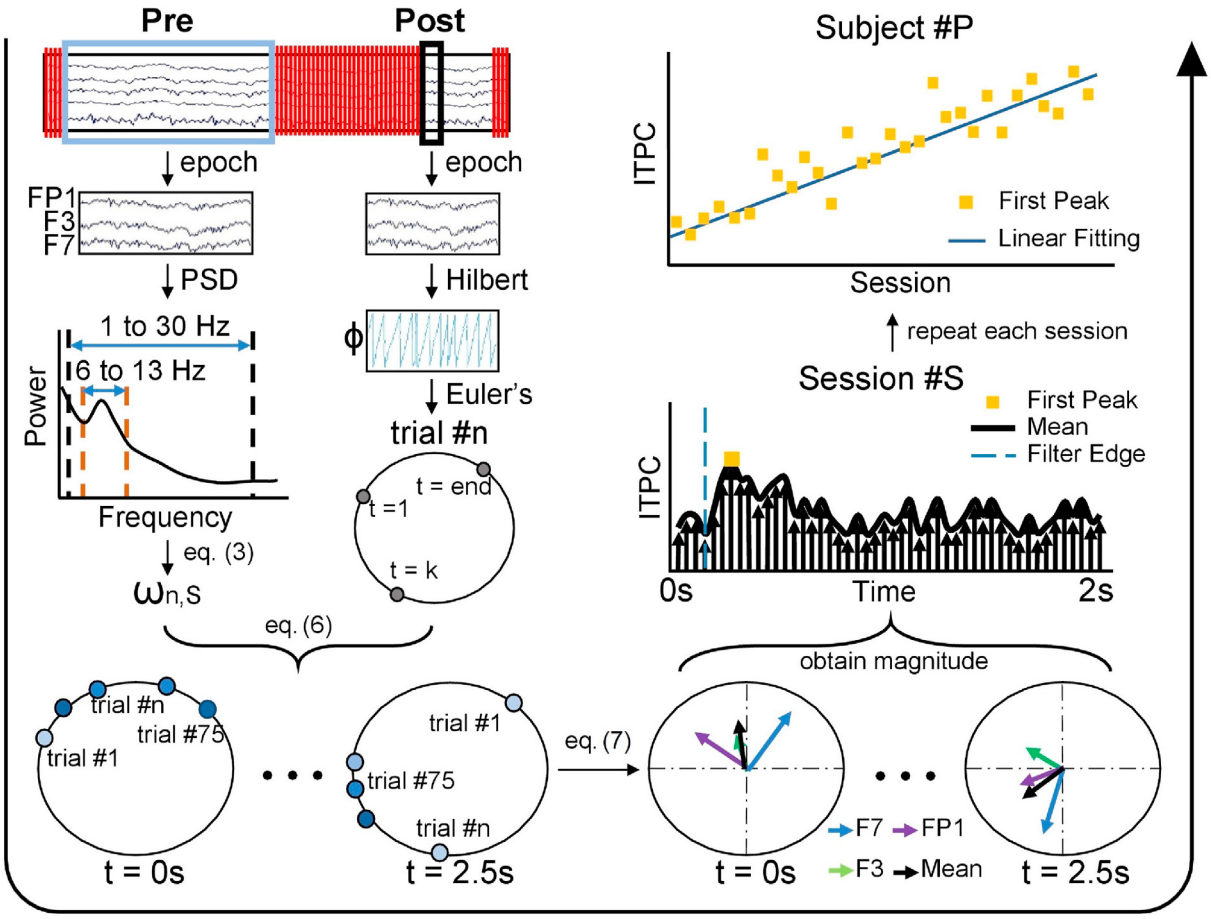

Fig. 3. Flowchart of trial-weighted inter-trial phase coherence (ITPC) calculation. Processing flow is indicated by the large black arrow which starts at the upper left and goes counterclockwise to the upper right. First, two datasets were generated, one **Pre** and one **Post** with respect to the TMS pulse train. The **Pre** data was used for the trial weight calculation and the **Post** segment was used for the post-stimulation phase calculation. For each pulse train, the trial weight, $\omega_{n,S}$, was calculated based on relative alpha power of the **Pre** segment. The phase of the **Post** segment was obtained by a Hilbert transform, shown in polar coordinates by applying Euler's formula. This process was repeated for each pulse train of one session, and the results of each pulse train were combined via Equation (6) resulting in the trial weighted-phases, shown as polar coordinates, from t = 0s to t = 2.5s post rTMS pulse train. In the figure, trials with greater weight are shown with darker blue, while a smaller trial weight is shown as lighter blue. Using Equation (7), the trial weighted ITPC was calculated for each electrode in a region (shown here is the target region including electrodes FP1, F3, and F7) and the mean of the ITPC was also calculated across the three electrodes. The magnitude of vectors (mean, black) were plotted in the time window $t = [0, 2]$ s and the first peak of ITPC ($ITPC^{max[1]}$) was taken to present the post-stimulation ITPC value for that session. Finally, we analyzed how this time series of $ITPC^{max[1]}$ changes across sessions for each subject #P, as shown in the upper right corner which uses a SYNC subject who has increasing phase entrainment as an example. (For interpretation of the references to colour in this figure legend, the reader is referred to the Web version of this article.)

relationship between $ITPC^{max[1]}$ and the corresponding independent variables which include stimulation frequency (IAF), relative quasi-alpha power $\bar{\alpha}_P$, session number of each treatment, and subject's treatment group (SYNC or UNSYNC). The fixed-effects in the model included stimulation frequency, relative quasi-alpha power, treatment group, session number, the interaction between treatment group and relative power, and the interaction between treatment group and session number. The subject difference was modeled by grouping variable *sub* as random-effects. Therefore, the final model is:

$$\ln\left(\frac{ITPC^{max[1]}}{1-ITPC^{max[1]}}\right) \sim stimf + (session + \bar{\alpha}_P)*condition + (1|sub) + \epsilon, \quad \ln\left(\frac{ITPC^{max[1]}}{1-ITPC^{max[1]}}\right) \in [0,1] \tag{9}$$

where $ITPC^{max[1]}$ refers to the first post-stimulation ITPC peak value for each session; *stimf* refers to the stimulation frequency for each session; *session* is the corresponding session number (e.g., the first treatment is 1); $\bar{\alpha}_P$ is the relative quasi-alpha power for each session; *condition* is the SYNC(1) or UNSYNC(-1) group; *sub* represents each subject (e.g., the first subject is 1). In addition, because the range of $ITPC^{max[1]}$ is between 0 and 1 ($ITPC \in [0, 1] \Rightarrow ITPC^{max[1]} \in [0, 1]$), the logit link function is applied in this linear model.

3. Results

Fifteen patients with treatment resistant depression (part of a double-blind clinical trial, see Material and Method Section) were enrolled and assigned randomly to either of the two treatment arms, SYNC (experimental treatment) or UNSYNC (active comparator) (see Table 1). A preferred phase of quasi-alpha EEG, defined as the phase at which a TMS pulse to left DLPFC evoked strongest activity in dorsal anterior cingulate cortex (dACC), was determined for every subject in a single session of combined fET (see S.1 in supplementary materials for details). Patients participated in 30

treatment sessions, only one session per work day for six weeks (extended to seven weeks if sessions were skipped). For these treatment sessions, participants were seated comfortably in an adjustable armchair with the EEG-rTMS setup (see Fig. 1). Every closed-loop EEG-rTMS treatment session (see Fig. 2) started with 5 min of resting state recording where an individual alpha frequency (IAF) and triggering threshold (RMSE) was determined (see S.4 in supplementary materials for details). The closed-loop EEG-rTMS treatment for one session lasted approximately 30 min, and patients received 75 pulse trains of rTMS, with 40 pulses per train over the left DLPFC at 120% of intensity relative to their individual motor threshold (see S.3 in supplementary materials for how motor threshold was determined). The interval between pulses in a pulse train was set to $\Delta t_{ipi} = 1/IAF$ (e.g., 125 ms for a patient with alpha frequency of 8 Hz) for both the SYNC and UNSYNC groups. For patients who were assigned to the group SYNC, the first TMS pulse in each train of 40 pulses was triggered at the individual's preferred phase, as determined from the initial fET session ($\varphi_{targ} = \varphi_{pre}$). For patients in the UNSYNC group, the preferred phase was not targeted, but instead the target phase was drawn randomly from a uniform distribution over the range $[0, 2\pi]$ for the first pulse in every rTMS pulse train ($\varphi_{targ} \sim U(0, 2\pi)$). The hardware setup and software used to administer the EEG-guided rTMS is described in more detail in S.2 of supplementary materials (also see Refs. [24,37].

3.1. SYNC patients show increased inter-trial phase coherence over sessions and decreased phase difference relative to the optimal phase for the therapeutic target

Fig. 4 shows examples of how the ITPC, for a given session, is estimated from the raw data for both SYNC and UNSYNC subjects. Post-stimulation, we observed an increase across sessions in the first ITPC peak (or $ITPC^{max[1]}$) around the stimulation site (left DLPFC; based on electrodes F3, FP1 and F7) for SYNC patients relative to the control group UNSYNC (Spearman's rank correlation coefficient, Table 3). Specifically, for the SYNC experimental group, three of seven subjects showed a statistically significant ($p < 0.05$) increase in the post-stimulation $ITPC^{max[1]}$ over sessions (see Table 3), suggesting that more days of treatment with phase synchronized rTMS was associated with increasingly greater post-stimulation alignment in quasi-alpha phase between trials. For the UNSYNC control group, this effect was observed for only one of eight subjects (see Table 3). Fig. 5 compares the changes in the post-stimulation $ITPC^{max[1]}$ for SYNC and UNSYNC groups both by session and by week. We see that five SYNC group subjects show an increase in quasi-alpha entrainment represented by positive $\Delta ITPC^{max}[1]$ between the first and last session (where the first session value was subtracted as baseline, see Fig. 5 (A)). Group level effects were tested with non-parametric tests. A two-sided Wilcoxon signed rank test was used to test the difference between the first and last session within each group, where the null hypothesis was that the difference between the first and last session comes from a distribution with zero median [54]. A Wilcoxon rank sum test was also used to test the difference between the first and last session across groups, with the null hypothesis being they come from the same population [54]. As there may be noise/variation in the measurement of each single treatment session, we also did a similar analysis by averaging sessions across week. This analysis was similar to the session comparison, except $\Delta ITPC^{max[1]}$ was calculated between the first and last week (where all sessions in a week were averaged and the ITPC of the first week was subtracted as baseline, see Fig. 5 (B)). The group level effect is the most significant ($p = 0.0059$) between SYNC and UNSYNC groups in the week comparison. This indicates that though the impact may be variable across individual days, EEG synchronized rTMS treatment is associated with greater post-stimulation quasi-alpha entrainment, compared to unsynchronized treatment, over the long-term across multiple sessions extending over weeks.

We also investigated the relationship between each subject's peak quasi-alpha entrainment phase (φ_{ent}) and their individual preferred phase that maximally engaged the ACC target (φ_{pre} from pre-treatment scan and φ_{post} from post-treatment scan). Here, φ_{ent} is the corresponding phase at the time when the first post-stimulation ITPC peak, $ITPC^{max[1]}$, was found (see Fig. 4, i.e., the entrainment phase calculated based on electrode F3 for subject #P09, #Session 18 is 316.4724°). Specifically, we looked at the difference, both at the beginning of the treatment and at the end of the six weeks, between the φ_{ent} and the phase eliciting the maximal response in the ACC target region. As mentioned earlier, the pre-treatment preferred phase (φ_{pre}) was determined using a simultaneous fET scan. We also performed a second post-treatment fET scan at the end of the six-week treatments to determine the preferred phase at that point (φ_{post}), since treatment itself could potentially affect the phase relationship between the TMS and the activity at the therapeutic target, namely the ACC. First, we obtained the corresponding φ_{ent} at the time that $ITPC^{max[1]}$ was detected for the treatments of the first and last week, where each week included 5 treatment sessions. Then the circular mean was calculated to represent the entrainment phase of the first ($\varphi_{ent,1^{st}}$) and last week ($\varphi_{ent,6^{th}}$). For the first week we computed the differences, for each subject, of $\varphi_{ent,1^{st}}$ and φ_{pre} computed pre-treatment, while for the last week we computed the differences of $\varphi_{ent,6^{th}}$ relative to φ_{post}. Fig. 5(C) and (D) show the results for each treatment group. For the SYNC group, 5 out of 7 subjects' phase differences (entrainment phase minus preferred target phase) decrease from the first to the last week, indicating that the entrainment phase and preferred target phase are converging over the treatment sessions. Conversely, in the UNSYNC group, we see this convergence in only 1 out of 6 subjects. Note that two UNSYNC subjects are excluded here because their post-treatment fET scans were not available. A Kruskal-Wallis test was used to test the null hypothesis that the phase difference in the first and last week in each group (SYNC vs UNSYNC) comes from the same distribution [55]. Treating the direction of the phase changes (clockwise vs counterclockwise) as different and considering the magnitude of the differences, we find we can reject the null hypothesis ($p = 0.0455$) at the 5% significance level. We performed a second test to investigate whether an increase/decrease of phase was different across the groups, regardless of the magnitude of the individual changes for each subject. We applied Fisher's exact test to Table 2 to test if there are nonrandom associations between the categorical findings of increase/decrease of phase difference in SYNC and UNSYNC groups. The result of Fisher's test is $p = 0.1026$, thus we cannot reject the null hypothesis of no nonrandom association between the categorical variables (SYNC vs UNSYNC) at the 5% significance level. This finding, together with the analysis taking the magnitude of the phase difference into account and the significant increase in entrainment over time, is consistent with an interpretation that there is a shift in phase that is induced in the SYNC group. Thus the individual entrainment phase appears to move toward the individual preferred phase, i.e., toward the phase associated with the strongest BOLD activation in the ACC after subjects received rTMS treatment synchronized to their quasi-alpha activity (mainly alpha activity).

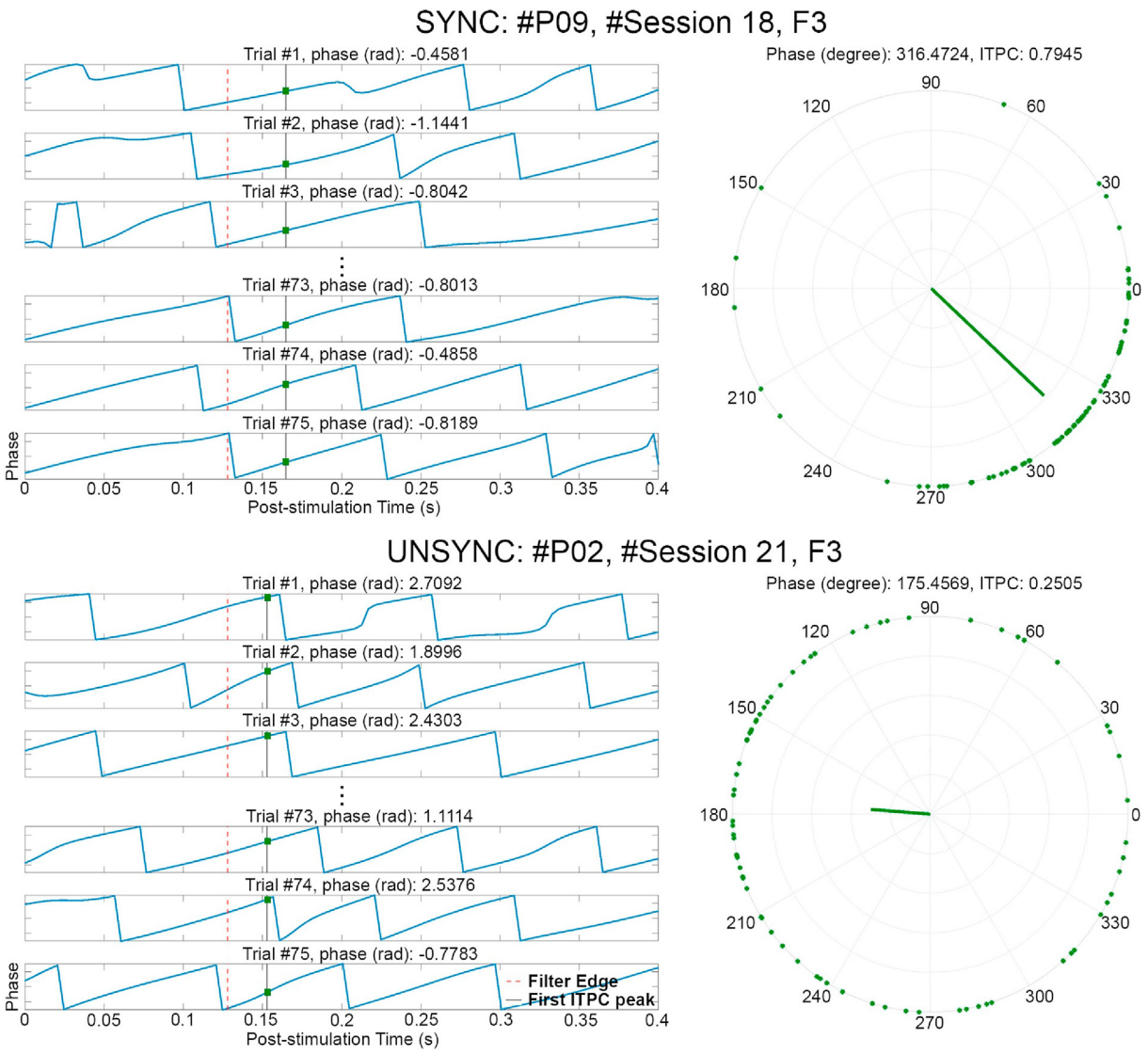

Fig. 4. Estimate of phase entrainment in the quasi-alpha band (6–13 Hz) at the target electrode (F3). One session from a SYNC subject (#P09, #Session 18) and one session from an UNSYNC subject (#P02, #Session 21) are presented. For each trial of a session, the phase of the **Post** stimulation segment was obtained via Hilbert transform after alpha-band filtering, with the phase value shown (blue line) in each subpanel on the left. $t = 0$ refers to the end of one rTMS pulse train and the red dashed line in each subpanel indicates the filter edge ($t = 0.128$s). The black solid line is the corresponding time point where the first post-stimulation ITPC peak ($ITPC^{max[1]}$) was detected (one value was calculated per session). The intersection (green dot) of the blue line and black line is the corresponding phase value of $ITPC^{max[1]}$. These points, across all trials of a session, are combined via Equation (5) resulting in the phase points shown as the green dots on the polar coordinates ($r = 1$) on the right. Using Equations (6) and (7), the trial weighted $ITPC^{max[1]}$ (green bar) is calculated for electrode F3 based on these points. In this example, the value of $ITPC^{max[1]}$ for this SYNC subject is two times greater ($ITPC^{max[1]} = 0.7945$) than this UNSYNC subject ($ITPC^{max[1]} = 0.2505$) indicating much greater entrainment on F3. (For interpretation of the references to colour in this figure legend, the reader is referred to the Web version of this article.)

3.2. Evidence for entrainment both locally over the stimulation site and distally over the therapeutic target

In support of our hypothesis, we found a significant group level effect, where $ITPC^{max[1]}$ increased across sessions only when rTMS was synchronized to individual preferred phase (SYNC group). Specifically, we observed a statistically significant effect of the interaction between the factors session-number (1–30) and treatment group (SYNC and UNSYNC) on $ITPC^{max[1]}$ as the dependent variable (generalized linear mixed effects model; $\beta = 0.0307$, $p = 0.0000$, $R^2 = 0.4329$; see Table 4). Fig. 6 (A) shows the marginal effect of session-number on $ITPC^{max[1]}$ for the SYNC group on the near target region which includes electrodes FP1, F7 and F3 ($ITPC^{max[1]}_{1^{st}} = 0.2980$, $ITPC^{max[1]}_{30^{th}} = 0.5182$, $\Delta ITPC^{max[1]} = 0.2202$; see Fig. 6 (A)). No significant effect was observed for an increasing session-number on $ITPC^{max[1]}$ for the UNSYNC group ($ITPC^{max[1]}_{1^{st}} = 0.3204$, $ITPC^{max[1]}_{30^{th}} = 0.3289$, $\Delta ITPC^{max[1]} = 0.0085$; see Fig. 6 (A)). No significant effects were found for stimulation frequency (IAF) or session-number and treatment group alone. Random effects covariance parameters are shown in Table 5. We conducted the same analysis as a function of the EEG channels used to compute the post-stimulation $ITPC^{max[1]}$ (e.g. contralateral to rTMS target, see Fig. 6 (B)). The $ITPC^{max[1]}$ increase across sessions ($\Delta ITPC^{max[1]}$) is largest near the rTMS targeted area and fades to be non-significant in the area contralateral to the rTMS target (see Fig. 6).

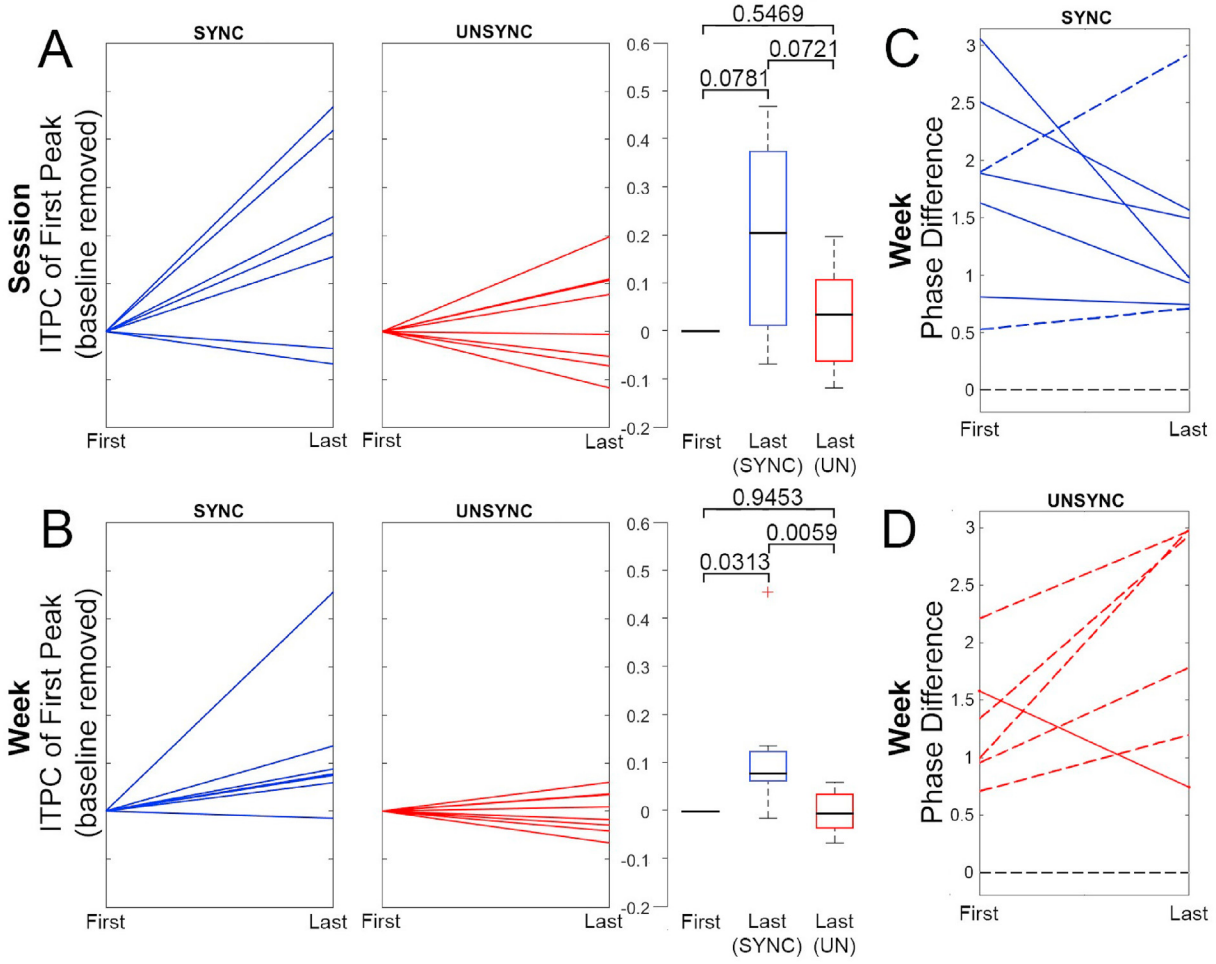

Fig. 5. Longitudinal changes in quasi-alpha entrainment for SYNC and UNSYNC groups. (A) Change in quasi-alpha entrainment between the first and last session, as measured by $ITPC^{max[1]}$. In each panel, blue represents the SYNC group and red represents the UNSYNC group. Each line is an individual subject (7 SYNC subjects and 8 UNSYNC subjects). Boxplots of data are shown on the right, together with the corresponding p-values of non-parametric tests of group level effects. Boxplots include the minimum, first (lower) quartile, median, third (upper) quartile, and maximum value of $\Delta ITPC^{max[1]}$, where the middle black line shows the median, the hinges represent first and third quartile and whiskers span from smallest to largest value in the data but reach out no further than 1.5 times the interquartile range. The data located outside of this range is indicated with a red cross. Panel (B) is similar to (A), except that pre- and post-treatment $ITPC^{max[1]}$ values are not derived from single sessions (i.e., the first and the last) but instead more robustly from an average across all sessions of one week (i.e., first vs last treatment week). (C) For the SYNC group (blue), this panel shows the difference ($\Delta\varphi \in [0, \pi]$) between the preferred phases (φ_{pre} and φ_{post}) and the phases at which ITPC peaked post-rTMS (see Fig. 3, center right) at two time points, before and after six weeks of treatment ($\varphi_{ent,1^{st}}$ presents the first week and $\varphi_{ent,6^{th}}$ presents the last week). Pre- and post-treatment preferred phase (φ_{pre} and φ_{post}) were obtained from two separate fET sessions acquired before (pre) and after (post) the full treatment course. Each line represents one subject, and seven subjects are included. A solid line indicates that the phase average of the last treatment week is closer to the preferred phase ($\left|\varphi_{ent,6^{th}} - \varphi_{post}\right| < \left|\varphi_{ent,1^{st}} - \varphi_{pre}\right|$), while a dashed line indicates that the phase average of the last week is further away from the preferred phase ($\left|\varphi_{ent,6^{th}} - \varphi_{post}\right| > \left|\varphi_{ent,1^{st}} - \varphi_{pre}\right|$). The black dashed line at phase difference $\Delta\varphi = 0$ at the bottom represents the point where post-rTMS ITPC peak phase is exactly at the individual's preferred phase ($\left|\varphi_{ent,6^{th}} - \varphi_{post}\right| = \left|\varphi_{ent,1^{st}} - \varphi_{pre}\right| = 0$). Panel (D) is similar to (C), except that the comparison is performed for the UNSYNC group (red) which includes six subjects with complete data. (For interpretation of the references to colour in this figure legend, the reader is referred to the Web version of this article.)

4. Discussion

In this paper, differences in the consistency of TMS phase-locked responses were evaluated using an ITPC comparison between patients in SYNC versus UNSYNC groups. We showed that $ITPC^{max[1]}$ observed after TMS pulse trains over the left DLPFC region significantly increased across treatment sessions for patients who received SYNC rTMS treatment, while it did not for patients in the active control condition UNSYNC. This result suggests that long-term continuous synchronized rTMS treatments over left DLPFC could lead to greater brain synchronization and entrainment in the targeted area in treatment-refractory MDD patients.

Despite rTMS being approved as a treatment for MDD, there continues to be a need to improve its efficacy [9,10,56]. In a recent study [57], reported on over 5000 patients treated at more than 100 private practice sites since FDA approval. Four to six weeks of daily rTMS resulted in 28–62% remission, and 58 to 83% response (over 50% reduction in symptoms). These results are impressive. However, around 20% of patients with medication-refractory depression do not respond to rTMS treatment as it is delivered today, which ignores the EEG phase of delivery and treatment length. As suggested by our prior studies using the fET system, synchronizing the TMS pulse to an individual's brain state over long periods of time is a method that is important for reaching deep areas such as the ACC,

Table 2
Number of patients in different phase change direction for each group.

Phase Difference	SYNC	UNSYNC
Closer	5	1
Farther	2	5

Table 3
Spearman correlation between post-stimulation trial weighted first post-stimulation ITPC peak ($ITPC^{max[1]}$) and Session; (***) indicates significant under a 99.9% confidence level; (**) indicates significant under a 99% confidence level; (*) indicates significant under a 95% confidence level; (.) indicates significant under a 90% confidence level.

Subject	Condition	P	p-value
P01	unsync	0.461 2	0.011 0(*)
P02	unsync	0.146 2	0.439 2
P03	unsync	0.067 0	0.724 4
P04	unsync	0.005 6	0.977 5
P05	unsync	−0.047 8	0.801 5
P06	unsync	−0.021 6	0.910 2
P07	unsync	−0.017 0	0.932 3
P08	unsync	−0.279 6	0.134 3
P09	sync	0.732 0	0.000 0(***)
P10	sync	0.458 5	0.011 5(*)
P11	sync	0.401 1	0.039 1(*)
P12	sync	0.311 2	0.094 4(.)
P13	sync	0.177 3	0.347 1
P14	sync	0.055 3	0.779 5
P15	sync	−0.143 0	0.449 2

so it may more efficiently engage the therapeutic target and affect the dynamics of the circuit that includes more than the DLPFC [24,34]. As this is a blinded ongoing trial, we are not yet able to test whether the entrainment effect seen here is linked to improved clinical response.

The observed increasing phase alignment over sessions may be attributable to neuroplasticity in the brain circuitry that gives rise to the prefrontal quasi-alpha oscillation [58,59]. We hypothesized that the phase of prefrontal alpha represents a gating mechanism [24,34,60,61], such that certain phases in the alpha are linked to states of greater excitability in which a higher dosage of TMS administered over the DLPFC will reach distal target structures such as the ACC. In practice, the EEG-rTMS system targeted frequencies in a wider range (6–13Hz) than is classically defined for alpha (8–12Hz). In system tests performed prior to the clinical trial using the alpha range, we found the system would not meet targeting specifications on many subjects. Since we did not know a-priori what the ideal frequency target would be for this population, and our mastoid montage optimized prefrontal alpha power partially at the expense of focality thus making our signal different from classically defined occipital alpha, it was decided to expand the range. As a result, our findings here suggest that there may be an increasing quasi-alpha entrainment to the stimulation. It is possible this may increase sensitivity/excitability at the target site at a certain preferred alpha phase for stimulation. Through this increasing alignment of phase across the stimulation sessions, the pulses may more frequently fall closer to the phase that is associated with a state of greater excitability, where treatment effects at distal target brain structures may also be greater.

Several studies have examined aspects of how the timing of stimulation relative to spectral phase may impact subsequent oscillatory dynamics. For example, spectral analysis by Ref. [62] suggested that single-pulse TMS induces a brief period of synchronized activity in the beta range (15–30 Hz) at the stimulation site. Ref. [63] have hypothesized that the entrainment of cerebral oscillations caused by exogenous stimulation can reset cortical oscillators, possibly enhancing neuroplasticity, normalizing cerebral blood flow, and ultimately ameliorating depressive symptoms so as to increase the efficiency of rTMS treatment. A behavioral study by Ref. [33] has shown that entrainment (phase-locking) of ongoing quasi-alpha neuronal oscillations to rhythmic stimuli is a potential mechanism for enhancing neuronal responses and perceptual sensitivity. Another study observed a sustained oscillatory echo in the left inferior frontal gyri (IFG) when stimulated at the beta frequency, with subjects having stronger entrainment showing more memory impairment [64]. Since our study is a double-blind clinical trial of MDD patients, the entrainment we observe can be examined relative to clinical improvement (such as higher rates of depression remission or response rate) and will provide a rigorous test of the hypothesis that entrainment effects are clinically meaningful.

Our results also show that the level of quasi-alpha entrainment post phase-locked rTMS treatment depends on whether rTMS was consistently locked to a specific phase in the cycle or not (i.e., SYNC or UNSYNC). Multiple studies have demonstrated that the modulation of brain excitability can depend on phase. Researchers in [15], for example, designed a close-loop system which combines different neuromodulation techniques (TMS and transcranial Alternating Current Stimulation (tACS)) and demonstrated that it can precisely hit the target phase to induce a phase dependent motor evoked potential (MEP) modulation with a phase lag. Researchers also found that cortico-cortical excitability is influenced by the phase of oscillatory activity at the time of the stimulus [65]. Using a closed-loop EEG-TMS system other researchers showed that the efficacy of TMS-induced plasticity in human motor cortex is determined by real-time EEG-defined excitability states [28]. Furthermore [66], reported that by applying controllable phase-synchronized rTMS with tACS, they were able to induce and stabilize neuro-oscillatory resting-state activity at targeted frequencies. It is noteworthy that these previous studies investigated effects that were tied to phase targets that were fixed and the same for all subjects (e.g. $+90^{\circ}$ and -90°). In contrast, here we selected a subject specific preferred phase by determining the phase that maximized BOLD response in the ACC. We found that there was some inter-subject variability in terms of which preferred phase elicited the strongest BOLD response to TMS. Our findings further complement the existing body of research, which has focused on short-term/immediate effects, with evidence that points to long-term entrainment effects.

Differences in brain synchronization changes, measured as post-stimulation quasi-alpha entrainment across treatment sessions in the targeted region, were found between SYNC and UNSYNC groups. For patients that received SYNC condition treatment (i.e.,

Table 4
Fixed effects coefficients (95% CIs).

Name	Estimate	SE	t-Stat.	DF	p-Value	Lower CI	Upper CI
(Intercept)	−0.392 9	0.337 1	−1.165 5	435	0.244 5	−1.055 6	0.269 7
Stimf	−0.040 5	0.025 6	−1.580 3	435	0.114 8	−0.090 9	0.009 9
$\bar{\alpha}_P$	−0.312 8	0.587 5	−0.532 3	435	0.594 8	−1.467 5	0.842 0
Session	0.001 3	0.003 8	0.348 7	435	0.727 5	−0.006 2	0.008 9
Condition	−0.135 5	0.314 5	−0.430 9	435	0.666 8	−0.753 7	0.482 7
$\bar{\alpha}_P$:condition	−1.517 4	0.825 7	−1.837 8	435	0.066 8	−3.140 1	0.105 4
session:condition	0.030 7	0.005 8	5.264 7	435	0.000 0	0.019 2	0.042 2

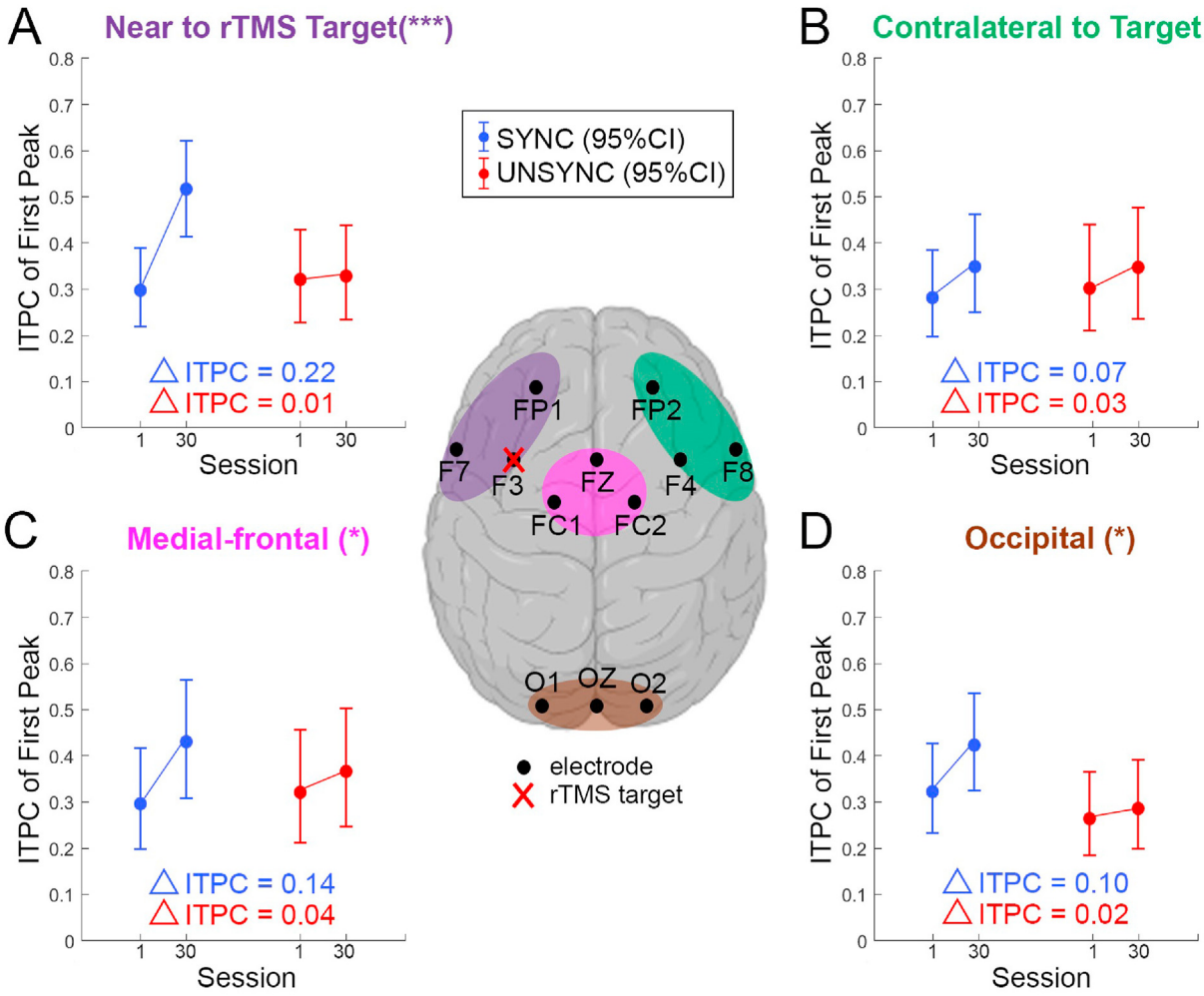

Fig. 6. Following the significant effect observed for the interaction between session and group (see Table 4), we here show the effect of treatment session separately for UNSYNC and SYNC groups (i.e., marginal effect) across four different regions of interest (ROIs) based on the GLMM prediction. The central figure defines the ROIs and the electrodes used in the analysis. All ROIs consist of three electrodes. rTMS is applied over the left DLPFC (over electrode F3) for all subjects. (A) The model prediction of changes in $ITPC^{max[1]}$ between the first and last session for SYNC and UNSYNC groups at the ROI near the rTMS target ROI, (B) contralateral to the target ROI, (C) in the medial-frontal ROI and (D) in the occipital ROI. The interaction-term of session and SYNC/UNSYNC group in the GLMM was highly significant in (A) (***, $p < 0.01$), significant in (C) and (D) (*, $0.01 < p < 0.05$) but not significant in (B).

onset of rTMS time-locked to preferred instead of random phase), the consistency of the TMS phase-locked response across trials increased as the number of treatment sessions increased. This was observed as an increase in the first ITPC peak value post-stimulation, $ITPC^{max[1]}$, across sessions. For patients in the UNSYNC group, no such effect was observed. Interestingly, on subject-level, one participant in the UNSYNC group showed statistically significant phase entrainment at a considerable correlation strength ($p = 0.011\,0$; $\rho = 0.46$). From reviewing demographic information and EEG data that are available at this stage of this double-blind study we have no explanation yet for this outlier. Other studies also investigated condition-specific brain synchronization differences after rTMS treatment with phase-focused measurements: [67] for example, found frequency-dependent brain connectivity changes in MDD-responders and MDD-non-responders after rTMS sessions using the Phase Locking Value (PLV). This result suggests that an increase in phase synchronization in the EEG after rTMS treatment could indicate which patients are more likely to respond with a clinically significant improvement in MDD-symptoms. Similar results have been shown elsewhere [68] based on another metric called Phase Lag Index (PLI). In a recent study [69], provided evidence for TMS-induced entrainment of alpha activity in occipital cortex using the ITPC metric. In accordance with the findings of these previous studies, we also found evidence in support of phase entrainment, specifically on a longer time scale of multi-week synchronized rTMS treatments.

Table 5
Random effects.

			Type	Estimate
Group: sub (15 Levels)	(Intercept)	(Intercept)	std	0.338 75
Group: Error	sqrt(Dispersion)	-	-	0.105 61

4.1. Limitations

While these findings are promising, there are a number of limitations to this study that should be considered when interpreting these findings more broadly. Specifically, while we found evidence for quasi-alpha phase entrainment in the condition SYNC, our study was not designed to determine whether any randomly chosen phase, rather than the predetermined subject-specific

preferred phase, would accomplish the same effect as long as it is kept fixed across the treatment sessions. Moreover, in a separate analysis of BOLD changes in ACC (manuscript in preparation), we found that there is a correlation between phase and the peak of BOLD activation at the group level, indicating it is possible that there is a general preferred phase which is not subject-specific. This would be consistent with previous findings from Ref. [28], which showed that across subjects, a negative μ-rhythm phase is associated with high corticospinal excitability, while positive μ-rhythm phase connects with low excitability. Future studies with adapted designs are needed to test whether rTMS can induce entrainment also if phase is fixed instead of tuned to the subject.

It is also noteworthy, as was mentioned above, that we defined the range of the individual alpha frequency between 6 and 13 Hz for this study, which is broader than the typical 8–12 Hz alpha range. This broadening may have incorporated high theta frequencies in addition to alpha, which is why we refer to the signal as "quasi-alpha" rather than alpha EEG. In fact, the two subjects who presented the highest effect size from the intervention had average target frequencies in the range of high theta frequencies, further suggesting not only prefrontal alpha oscillation but other physiologically meaningful oscillatory activities might have been included, which requires further investigation. Another limitation of this study is our relatively small sample size, and future studies replicating these results in larger samples are warranted. In addition, the patients receiving rTMS treatment continued to take their medication during the experiment. This was consistent across treatment arms but could conceivably influence patients' brain activity. In this study, we measured the first ITPC peak after rTMS offset to index and track brain synchronization across sessions. Future research could include other non-linear measurements like PLV or complexity analysis such as Higuchi fractal dimension (FD) and Lempel-Ziv Complexity. In fact, several studies have shown brain connectivity differences in MDD-responders after receiving rTMS treatment [67] and EEG complexity differences after rTMS between MDD-responders and non-responders based on FD [70,71] or Lempel-Ziv complexity [72].

An additional limitation is the selection of the right mastoid as the reference. Prior to the start of the clinical trial, multiple re-referencing methods were considered, including Laplacian, common average reference (CAR), and mastoids. Preliminary analyses indicated choosing the right mastoid provided the most stable alpha signal for system targeting. This provided an increase in SNR at the possible cost of being less certain if the quasi-alpha oscillation was primarily frontal, driven by posterior regions due to volume conduction, or mixed with oscillation in the motor area. While initial analyses comparing the phase of occipital and parietal regions to the phase of F3 suggest these more posterior regions are not the primary drivers of the frontal quasi-alpha signal studied, it is possible that this prefrontal oscillation is mixed with oscillations near motor area for several subjects. More investigation into optimized brain region and EEG signal targets, referencing schemes, and motor area is required (see S.10 in supplemental material). There is also a need for additional sham control conditions in TMS studies: TMS is a considerable source of sensory stimulation and sham-based control conditions are important so that findings in TMS-based experiments can be interpreted correctly and potential confounds can be ruled out [73,74]. During the original experimental design, an additional control condition that included sham TMS was considered, but we were unable to practically add additional arms to the study. Future experiments must include sham-based controls to rule out any potential confounds from the sensory stimulation associated with TMS. Though hypothetical, it is also possible the most relevant brain activity changes after rTMS occurred during the first 128 ms of EEG data immediately after the TMS pulse train; then we could have missed them as this time window was not included in our ITPC analysis due to the noise induced by bandpass filtering on each TMS pulse train segment. Novel and more powerful signal processing methods would be required to study relevant effects in these time windows. Finally, once our double-blind clinical trial is completed, clinical results on changes in depression scores should be included and compared.

5. Conclusions

To our knowledge, this is the first study to track changes in brain synchronization reflecting phase entrainment at 6–13 Hz across multiple weeks of rTMS treatments (6–7 weeks of 30 sessions). The observed increase in brain synchronization across treatments suggests that the efficacy of rTMS may be improved with synchronized rTMS pulse triggering. Moreover, combining fET and EEG-rTMS proved to be valuable for exploring the physiological and therapeutic effects of phase-synchronized stimulation in patients with MDD, especially those with treatment-refractory depression.

CRediT authorship contribution statement

Josef Faller: Conceptualization, Methodology, Software, Writing – original draft. **Jayce Doose:** Conceptualization, Investigation, Data curation, Writing – original draft, Writing – review & editing. **Xiaoxiao Sun:** Methodology, Formal analysis, Writing – original draft, Writing – review & editing, Visualization. **James R. McIntosh:** Conceptualization, Methodology, Software, Data curation, Writing – review & editing. **Golbarg T. Saber:** Conceptualization, Methodology, Data curation. **Yida Lin:** Software. **Joshua B. Teves:** Investigation, Data curation. **Aidan Blankenship:** Investigation, Data curation. **Sarah Huffman:** Investigation. **Robin I. Goldman:** Conceptualization, Methodology, Writing – review & editing, Funding acquisition, Project administration, Supervision. **Mark S. George:** Conceptualization, Methodology, Writing – review & editing, Funding acquisition, Project administration, Supervision. **Truman R. Brown:** Conceptualization, Methodology, Writing – review & editing, Funding acquisition, Project administration, Supervision. **Paul Sajda:** Conceptualization, Methodology, Writing – original draft, Writing – review & editing, Funding acquisition, Project administration, Supervision, All persons who meet authorship criteria are listed as authors, and all authors certify that they have participated sufficiently in the work to take public responsibility for the content, including participation in the concept, design, analysis, writing, or revision of the manuscript.

Acknowledgments

This work was funded by the National Institute of Mental Health (MH106775) and a Vannevar Bush Faculty Fellowship from the US Department of Defense (N00014-20-1-2027). We would like to thank Spiro P. Pantazatos for reviewing and providing feedback on the manuscript draft. We would like to thank Daniel Cook for his help with initial data collection with closed-loop EEG-rTMS. We would like to thank Michael Milici for his help with building the safety circuit box and ActiChamp testing. We would like to thank DeeAnn Guo for her help with ActiChamp testing and initial EEG data collection.

Appendix A. Supplementary data

Supplementary data to this article can be found online at https://doi.org/10.1016/j.brs.2022.02.008.

References

[1] George MS, Nahas Z, Molloy M, Speer AM, Oliver NC, Li X-B, Arana GW, Risch SC, Ballenger JC. A controlled trial of daily left prefrontal cortex TMS for treating depression. Biol Psychiatr 2000;48(10):962–70.

[2] Rodriguez-Martin JL, Barbanoj JM, Schlaepfer TE, Clos SS, Perez V, Kulisevsky J, Gironell A. Transcranial magnetic stimulation for treating depression. Cochrane Database Syst Rev 2002;(2).

[3] Kobayashi M, Pascual-Leone A. Transcranial magnetic stimulation in neurology. Lancet Neurol 2003;2(3):145–56.

[4] Hallett M. Transcranial magnetic stimulation: a primer. Neuron 2007;55(2):187–99.

[5] George MS, Lisanby SH, Avery D, McDonald WM, Durkalski V, Pavlicova M, Anderson B, Nahas Z, Bulow P, Zarkowski P, et al. Daily left prefrontal transcranial magnetic stimulation therapy for major depressive disorder: a sham-controlled randomized trial. Arch Gen Psychiatr 2010;67(5):507–16.

[6] Pascual-Leone A, Walsh V. 11 - transcranial magnetic stimulation. In: Toga AW, Mazziotta JC, editors. Brain mapping: the methods. second ed. Academic Press; 2002. p. 255–90. San Diego, second edition edition.

[7] Walsh V, Pascual-Leone A. Transcranial magnetic stimulation: a neurochronometrics of mind. MIT press; 2003.

[8] Sliwinska MW, Vitello S, Devlin JT. Transcranial magnetic stimulation for investigating causal brain-behavioral relationships and their time course. JoVE: JoVE 2014;(89).

[9] O'Reardon JP, Solvason HB, Janicak PG, Sampson S, Isenberg KE, Nahas Z, McDonald WM, Avery D, Fitzgerald PB, Loo C, et al. Efficacy and safety of transcranial magnetic stimulation in the acute treatment of major depression: a multisite randomized controlled trial. Biol Psychiatr 2007;62(11):1208–16.

[10] Markowitz JC, Rosenbaum JF, Thase ME, Gelenberg AJ, Freeman CMP. Practice guideline for the treatment of patients with major depressive disorder. third ed. Washington, DC: American Psychiatric Association; 2010.

[11] Woźniak-Kwaśniewska A, Szekely D, Aussedat P, Bougerol T, David O. Changes of oscillatory brain activity induced by repetitive transcranial magnetic stimulation of the left dorsolateral prefrontal cortex in healthy subjects. Neuroimage 2014;88:91–9.

[12] George MS, Ketter TA, Post RM. Prefrontal cortex dysfunction in clinical depression. Depression 1994;2(2):59–72.

[13] Fox P, Ingham R, George MS, Mayberg H, Ingham J, Roby J, Martin C, Jerabek P. Imaging human intra-cerebral connectivity by PET during TMS. Neuroreport 1997;8(12):2787–91.

[14] Mayberg HS, Brannan SK, Mahurin RK, Jerabek PA, Brickman JS, Tekell JL, Silva JA, McGinnis S, Glass TG, Martin CC, et al. Cingulate function in depression: a potential predictor of treatment response. Neuroreport 1997;8(4):1057–61.

[15] Raco V, Bauer R, Tharsan S, Gharabaghi A. Combining TMS and tACS for closed-loop phase-dependent modulation of corticospinal excitability: a feasibility study. Front Cell Neurosci 2016;10:143.

[16] Drysdale AT, Grosenick L, Downar J, Dunlop K, Mansouri F, Meng Y, Fetcho RN, Zebley B, Oathes DJ, Etkin A, et al. Erratum: resting-state connectivity biomarkers define neurophysiological subtypes of depression. Nat Med 2017;23(2):264.

[17] Barbas H, Ghashghaei H, Rempel-Clower N, Xiao D. Anatomic basis of functional specialization in prefrontal cortices in primates. Handb Neuropsychol 2002;7:1–28.

[18] Rushworth MF, Noonan MP, Boorman ED, Walton ME, Behrens TE. Frontal cortex and reward-guided learning and decision-making. Neuron 2011;70(6):1054–69.

[19] Medalla M, Barbas H. The anterior cingulate cortex may enhance inhibition of lateral prefrontal cortex via m2 cholinergic receptors at dual synaptic sites. J Neurosci 2012;32(44):15611–25.

[20] Caspers J, Mathys C, Hoffstaedter F, Südmeyer M, Cieslik EC, Rubbert C, Hartmann CJ, Eickhoff CR, Reetz K, Grefkes C, et al. Differential functional connectivity alterations of two subdivisions within the right dlPFC in Parkinson's disease. Front Hum Neurosci 2017;11:288.

[21] Hinkley LB, Vinogradov S, Guggisberg AG, Fisher M, Findlay AM, Nagarajan SS. Clinical symptoms and alpha band resting-state functional connectivity imaging in patients with schizophrenia: implications for novel approaches to treatment. Biol Psychiatr 2011;70(12):1134–42.

[22] Klimesch W. Alpha-band oscillations, attention, and controlled access to stored information. Trends Cognit Sci 2012;16(12):606–17.

[23] Sadaghiani S, Scheeringa R, Lehongre K, Morillon B, Giraud A-L, d'Esposito M, Kleinschmidt A. Alpha-band phase synchrony is related to activity in the fronto-parietal adaptive control network. J Neurosci 2012;32(41):14305–10.

[24] George M, Saber G, McIntosh J, Doose J, Faller J, Lin Y, Moss H, Goldman R, Sajda P, Brown T. Combined TMS-EEG-fMRI. the level of TMS-evoked activation in anterior cingulate cortex depends on timing of TMS delivery relative to frontal alpha phase. Brain Stimul.: Basic, Trans. Clin. Res. Neuromodulation 2019;12(2):580.

[25] Busch NA, Dubois J, VanRullen R. The phase of ongoing EEG oscillations predicts visual perception. J Neurosci 2009;29(24):7869–76.

[26] Milton A, Pleydell-Pearce CW. The phase of pre-stimulus alpha oscillations influences the visual perception of stimulus timing. Neuroimage 2016;133:53–61.

[27] Ronconi L, Busch NA, Melcher D. Alpha-band sensory entrainment alters the duration of temporal windows in visual perception. Sci Rep 2018;8(1):1–10.

[28] Zrenner C, Desideri D, Belardinelli P, Ziemann U. Real-time EEG-defined excitability states determine efficacy of TMS-induced plasticity in human motor cortex. Brain Stimul. 2018;11(2):374–89.

[29] Zrenner B, Zrenner C, Gordon PC, Belardinelli P, McDermott EJ, Soekadar SR, Fallgatter AJ, Ziemann U, Müller-Dahlhaus F. Brain oscillation-synchronized stimulation of the left dorsolateral prefrontal cortex in depression using real-time EEG-triggered TMS. Brain Stimul. 2020;13(1):197–205.

[30] Torrecillos F, Falato E, Pogosyan A, West T, Di Lazzaro V, Brown P. Motor cortex inputs at the optimum phase of beta cortical oscillations undergo more rapid and less variable corticospinal propagation. J Neurosci 2020;40(2):369–81.

[31] Thut G, Veniero D, Romei V, Miniussi C, Schyns P, Gross J. Rhythmic TMS causes local entrainment of natural oscillatory signatures. Curr Biol 2011;21(14):1176–85.

[32] Wagner J, Makeig S, Hoopes D, Gola M. Can oscillatory alpha-gamma phase-amplitude coupling be used to understand and enhance TMS effects? Front Hum Neurosci 2019;13:263.

[33] Samaha J, Iemi L, Haegens S, Busch NA. Spontaneous brain oscillations and perceptual decision-making. Trends Cognit Sci 2020;24(8).

[34] Saber G, McIntosh J, Doose J, Faller J, Lin Y, Moss H, Goldman R, George M, Sajda P, Brown T. Level of TMS-evoked activation in anterior cingulate cortex depends on timing of TMS delivery relative to frontal alpha phase. Proc. Int. Soc. Magn. Reson. Med. 2018;26:4518.

[35] Papenberg G, Hämmerer D, Müller V, Lindenberger U, Li S-C. Lower theta inter-trial phase coherence during performance monitoring is related to higher reaction time variability: a lifespan study. Neuroimage 2013;83:912–20.

[36] van Diepen RM, Mazaheri A. The caveats of observing inter-trial phase-coherence in cognitive neuroscience. Sci Rep 2018;8(1):1–9.

[37] Faller J, Lin Y, Doose J, Saber G T, McIntosh J, Teves J, Goldman R, George M, Sajda P, Brown T. An EEG-fMRI-TMS instrument to investigate bold response to eeg guided stimulation. 2019. p. 1054–7.

[38] Pantazatos Spiro P, Mclntosh James R, Saber Golbarg T, Sun Xiaoxiao, Doose Jayce, Faller Josef, et al. Functional and effective connectivity between dorsolateral prefrontal and subgenual anterior cingulate cortex depends on the timing of transcranial magnetic stimulation relative to the phase of prefrontal alpha EEG. bioRxiv 2022. https://doi.org/10.1101/2022.02.14.480466. Submitted for publication.

[39] Jasper HH. The ten-twenty electrode system of the International Federation. Electroencephalogr Clin Neurophysiol 1958;10:370–5.

[40] Sekiguchi H, Takeuchi S, Kadota H, Kohno Y, Nakajima Y. Tms-induced artifacts on EEG can be reduced by rearrangement of the electrode's lead wire before recording. Clin Neurophysiol 2011;122(5):984–90.

[41] Kothe C. Lab streaming layer (LSL). https://github.com/sccn/labstreaminglayer; 2014a. Accessed on October.

[42] Kothe C, Brunner C. Lab streaming layer (LSL): a system for unified collection of measurement time series in research experiments. https://github.com/sccn/xdf; 2014b. Accessed on October.

[43] Makeig S, Bell AJ, Jung T-P, Sejnowski TJ. Independent component analysis of electroencephalographic data. In: Advances in neural information processing systems; 1996. p. 145–51.

[44] Viola FC, Thorne J, Edmonds B, Schneider T, Eichele T, Debener S. Semi-automatic identification of independent components representing EEG artifact. Clin Neurophysiol 2009;120(5):868–77.

[45] Delorme A, Makeig S. EEGLAB: an open source toolbox for analysis of single-trial EEG dynamics including independent component analysis. J Neurosci Methods 2004;134(1):9–21.

[46] McIntosh JR, Sajda P. Estimation of phase in EEG rhythms for real-time applications. J Neural Eng 2020;17(3):034002.

[47] Niso G, Bruña R, Pereda E, Gutiérrez R, Bajo R, Maestú F, Del-Pozo F. HERMES: towards an integrated toolbox to characterize functional and effective brain connectivity. Neuroinformatics 2013;11(4):405–34.

[48] Rahman M. Integral equations and their applications. WIT press; 2007.

[49] Mo Y, Qian T, Mai W, Chen Q. The AFD methods to compute Hilbert transform. Appl Math Lett 2015;45:18–24.

[50] Corder GW, Foreman DI. Nonparametric statistics: a step-by-step approach. John Wiley & Sons; 2014.

[51] Daniel WW, et al. Applied nonparametric statistics. second ed. Boston: PWS-Kent Pub; 1990.

[52] Breslow NE, Clayton DG. Approximate inference in generalized linear mixed models. J Am Stat Assoc 1993;88(421):9–25.

[53] Jiang J. Linear and generalized linear mixed models and their applications. Springer Science & Business Media; 2007.

[54] Wilcoxon F. Individual comparisons by ranking methods. In: Breakthroughs in statistics. Springer; 1992. p. 196–202.

[55] Kruskal WH, Wallis WA. Use of ranks in one-criterion variance analysis. J Am Stat Assoc 1952;47(260):583–621.

[56] Anderson RJ, Hoy KE, Daskalakis ZJ, Fitzgerald PB. Repetitive transcranial magnetic stimulation for treatment resistant depression: Re-establishing connections. Clin Neurophysiol 2016;127(11):3394–405.

[57] Sackeim HA, Aaronson ST, Carpenter LL, Hutton TM, Mina M, Pages K, Verdoliva S, West WS. Clinical outcomes in a large registry of patients with

major depressive disorder treated with Transcranial Magnetic Stimulation. J Affect Disord 2020;277:65–74.
[58] Lewis DA. Neuroplasticity of excitatory and inhibitory cortical circuits in schizophrenia. Dialogues Clin Neurosci 2009;11(3):269.
[59] Liu KK, Bartsch RP, Lin A, Mantegna RN, Ivanov PC. Plasticity of brain wave network interactions and evolution across physiologic states. Front Neural Circ 2015;9:62.
[60] Veniero D, Brignani D, Thut G, Miniussi C. Alpha-generation as basic response-signature to transcranial magnetic stimulation (TMS) targeting the human resting motor cortex: a TMS/EEG co-registration study. Psychophysiology 2011;48(10):1381–9.
[61] Kundu B, Johnson JS, Postle BR. Prestimulation phase predicts the TMS-evoked response. J Neurophysiol 2014;112(8):1885–93.
[62] Paus T, Sipila P, Strafella A. Synchronization of neuronal activity in the human primary motor cortex by transcranial magnetic stimulation: an EEG study. J Neurophysiol 2001;86(4):1983–90.
[63] Leuchter AF, Cook IA, Jin Y, Phillips B. The relationship between brain oscillatory activity and therapeutic effectiveness of transcranial magnetic stimulation in the treatment of major depressive disorder. Front Hum Neurosci 2013;7:37.
[64] Hanslmayr S, Matuschek J, Fellner M-C. Entrainment of prefrontal beta oscillations induces an endogenous echo and impairs memory formation. Curr Biol 2014;24(8):904–9.
[65] Desideri D, Belardinelli P, Zrenner C, Ziemann U. Cortico-cortical excitability is influenced by the phase of oscillatory activity at the time of the stimulus. Brain Stimul.: Basic, Trans. Clin. Res. Neuromodulation 2017;10(2):491.
[66] Hosseinian T, Yavari F, Biagi MC, Kuo M-F, Ruffini G, Nitsche MA, et al. External induction and stabilization of brain oscillations in the human. Brain Stimul. 2021;14(3). https://doi.org/10.1016/j.brs.2021.03.011.
[67] Zuchowicz U, Wozniak-Kwasniewska A, Szekely D, Olejarczyk E, David O. EEG phase synchronization in persons with depression subjected to transcranial magnetic stimulation. Front Neurosci 2019;12:1037.
[68] Olbrich S, Tränkner A, Chittka T, Hegerl U, Schönknecht P. Functional connectivity in major depression: increased phase synchronization between frontal cortical EEG-source estimates. Psychiatr Res Neuroimaging 2014;222(1–2):91–9.
[69] Lin Y-J, Shukla L, Dugué L, Valero-Cabré A, Carrasco M. TMS entrains occipital alpha activity: individual alpha frequency predicts the strength of entrained phase-locking. bioRxiv; 2021.
[70] Akar SA, Kara S, Agambayev S, Bilgiç V. Nonlinear analysis of EEGs of patients with major depression during different emotional states. Comput Biol Med 2015;67:49–60.
[71] Bachmann M, Päeske L, Kalev K, Aarma K, Lehtmets A, Ööpik P, Lass J, Hinrikus H. Methods for classifying depression in single channel EEG using linear and nonlinear signal analysis. Comput Methods Progr Biomed 2018;155:11–7.
[72] Arns M, Cerquera A, Gutiérrez RM, Hasselman F, Freund JA. Non-linear EEG analyses predict non-response to rTMS treatment in major depressive disorder. Clin Neurophysiol 2014;125(7):1392–9.
[73] Siebner H, Conde V, Tomasevic L, Thielscher A, Bergmann T. Distilling the essence of TMS-evoked EEG potentials (TEPS): a call for securing mechanistic specificify and experimental rigor. Brain Stimul. 2019;12(4):1051–4.
[74] Belardinelli P, Biabani M, Blumberger D, Bortoletto M, Casarotto S, David O. Reproducability in TMS-EEG studies: a call for data sharing, standard procedures and effective experimental control. Brain Stimul. 2019;12(3):787–90.